TÜBİTAK

Turk J Elec Eng & Comp Sci, Vol.19, No.3, 2011, © TÜBİTAK
doi:10.3906/elk-0911-245

# A complete motor protection algorithm based on PCA and ann: A real time study

**Okan ÖZGÖNENEL*, Turgay YALÇIN**
*Department of Electrical and Electronic Engineering, Ondokuz Mayıs University, 55139, Kurupelit, Samsun-TURKEY*
*e-mails: okanoz@omu.edu.tr, yalcnturgay@yahoo.com.tr*

Received: 04.11.2009

**Abstract**

*Protection of an induction motor (IM) against possible faults, such as a stator winding fault, due to thermal deterioration, rotor bar and bearing failures, is very important in environments in which it is used intensively, as in industry as an actuator. In this work, a real time digital protection algorithm based on principal component analysis (PCA) and neural network method is presented for induction motors. The proposed protection algorithm covers internal winding faults (also known as stator faults), broken rotor bar faults, and bearing faults. Many laboratory experiments have been performed on a specially designed induction motor to evaluate the performance of the suggested protection algorithm. The hybrid protection algorithm described in this paper uses is based on a three phase rms supply. These currents are first preprocessed by PCA to extract distinctive features called residuals. The calculated residuals are applied to a feed-forward back-propagation neural network as input vectors for decision making. Outputs of the network are signals denoting winding fault, rotor bar fault, bearing fault, and normal operation. The proposed algorithm is implemented by using Matlab$^{TM}$ and C++ with a NI-DAQ data acquisition board.*

**Key Words:** *PCA, induction motor (IM), faults, neural network*

## 1. Introduction

The induction motor is one of the single most common electromechanical energy conversion devices. It is a critical component in production processes and is widely used in domestic, commercial, and industrial motion control devices and systems. An induction motor is considered inherently reliable due to its time-tested robustness, relatively simple design and construction. However, it often faces various stresses during operation, and might lead to many modes of failure.

Statistics have shown that despite reliability and construction simplicity, motor annual failure rate is conventionally estimated at 3–5% per year, and in extreme cases, up to 12% in pulp and paper industry [1]. A

*Corresponding author: Department of Electrical and Electronic Engineering, Ondokuz Mayıs University, 55139, Kurupelit, Samsun-TURKEY

method for condition monitoring and reliable protection has become necessary in order to avoid catastrophic failures (breakdowns) to ensure long motor life. Monitoring reduces maintenance costs and prevents unscheduled downtimes. Therefore there has been a substantial amount of research to provide new condition monitoring techniques for AC induction motors.

We divide faults in into three main categories: stator winding faults, broken rotor bar problems, and bearing problems. Turn-to-turn and turn-to-earth faults in an IM stator winding lead to asymmetry between the three phases, causing undesirable motor behavior and heat. Heat generation in the stator windings, in turn, causes insulation breakdown, followed by stator winding fault. This is nearly 30–40% of the total motor failures. Generally the term "stator faults" is used for IMs and they can be classified into two different categories: laminations or frame faults and stator winding faults [2].

There are recent studies regarding with IM protection in literature. These studies are almost related to thermal model (behavior) of the motor and motor current signature analysis (MCSA).

Thermal model and its applications are applied in [3]. Different stages of motor operations such as overload, locked rotor, too frequent or prolonged acceleration are studied. Similarly, thermal modeling for overload protection and variable ground fault protection are taken into account in [4]. It is stressed in References [3] and [4] that usage of non-organic insulation materials such as fiberglass and silicon resins provide improved dielectric capabilities of the motor insulation over legacy materials such as cotton and varnish; at the same time these are more susceptible to excessive heating. A new IM protection method is presented by using programmable logical controller (PLC) in Reference [4]. The voltages, currents, speed, and temperature of the IM are monitored and warning messages are displayed at the computer screen.

Several interesting diagnostic techniques have been introduced in the literature to early-identify the type of fault [5–9]. However, to the present authors' knowledge, most of these techniques do not offer the ability to identify the specific faulty phase unless the neutral point is accessible or intrusive sensors are installed inside the machine itself [10].

One of the biggest problems in IM failure issue from the bearings, accounting for over 40% of all faults. A successful bearing condition monitoring scheme must be able to detect location of faults and their severity levels. Bearing faults have been traditionally detected at incipient stage through vibration and stator current monitoring. Experimental results reveal the nature of vibration harmonic frequency bands which do not have any relationship to characteristic frequencies that have previously been used for bearing fault identification [11].

Another fault in IMs is broken rotor bar failure, but is not very common. The classical approach used in industry to detect of rotor bar failure in IMs is based on analysis of stator current in the steady state, using two harmonic components placed around the main frequency component at distances $+2sf$ and $-2sf$ (side band harmonics), where $f$ is the main frequency and $s$ is the slip [12]. This approach has been widely used due to its inherent advantages. However, it has some drawbacks for diagnosis purposes. One is load dependence, for amplitude of the current components depends on the load connected to the motor and on the inertia of the connected motor-load system. If the machine is unloaded, this approach is unsuitable as the slip will be approximately zero, and the frequencies associated with the broken rotor bars will overlap the supply frequency. Another problem with this method is that frequencies similar to those used for the rotor bar breakage detection can be generated by other sources, such as low frequency oscillating torque loads, voltage fluctuations, or bearing faults [13]. Several interesting methods based on the steady state analysis can avoid some of these disadvantages [14–15], but most of them analyze other magnitudes [16–18].

As stated above, among the most important fault detection based on motor current is the motor current

signature analysis (MCSA). This method relies on the interpretation of the frequency components in the stator current spectrum. Another successful fault detection method based on MCSA is the Park's vector approach. It is based on the identification of a specified current pattern obtained from the transformation of the three phase stator currents to an equivalent two phase system [19–20].

Artificial neural networks (ANNs) is one among several soft computing techniques that be used to perform induction motor fault detection. ANNs have advantages such as flexibility to learn and do not need a precise mathematical model of the motor.

Methods proposed by other authors are focused on the analysis of wavelet coefficients or use other mathematical techniques such as wavelet ridge. Other works convolute the start-up current signal with a Gaussian wavelet, which was centered on a particular frequency, to extract the evolution of the fault components [18, 21–22].

This work is an extended study of paper [23] and presents a complete real time induction motor protection algorithm based on dynamical principal component analysis (PCA). In [13], the authors tried to identify (only) stator winding fault (so-called inter-turn faults or insulation faults) based on PCA and RBF based neural network in Matlab$^{TM}$ environment.

In this work, a combination of dynamical PCA approach and subsequently a feed-forward back propagation neural network approach are used for MCSA to detect stator insulation failures (internal faults), broken rotor bar, and bearing faults. Dynamical PCA is used for feature vector extraction by using rms values of stator line currents. A Feed forward back propagation neural network is used for fault identification purpose. The future vectors produced by using PCA have been used to train the neural network both off-line net training and on-line fault identification procedure. The overall protection scheme needs only 3 current sensors to implement the proposed hybrid algorithm and does not require thermal sensors unlike the recent References [2], [3] and [4]. A specially designed four-pole, 1000 VA, 50 Hz induction motor is used for laboratory experiments to validate the proposed techniques.

Remainder of this paper is organized as follows. Section 2 gives the details of PCA algorithm and its usage, SVD calculation, and error vector calculation procedures. Section 3 gives the details of ANN structure for decision making unit. Section 4 presents real time experiments and performance of the overall hybrid protection scheme. Finally, the Conclusion gives some concluding remarks.

## 2. Background of principal component analysis

Principal component is defined as a linear transformation of the original variables, which are normally correlated, into a new set of variables that are orthogonal to one another. The basic goal in PCA dimensionally reduces the data. This is done in the mean square sense. Such a reduction in dimension decreases the calculation time and removes affects of the noise. The main idea behind principal component analysis is to represent multidimensional data with fewer numbers of variables retaining main features of the data. It is inevitable that by reducing dimensionality some features of the data will be lost. It is hoped that these lost features are comparable with the "noise-fault" and they do not tell much about underlying population.

The PCA method tries to project multidimensional data to a lower dimensional space retaining as much as possible variability of the data. PCA is also a useful statistical technique having found application in fields such as face recognition and image compression, and is a common technique for finding patterns in data of high dimension [24].

Main ideas of PCA are reducing dimensionality without loosing much information, finding a canonical representation of the data, and preserving variance of data. The following procedures ***A*** and ***B*** are useful for understanding the concept of the PCA algorithm.

**A)** Projecting a point (data vector) into a lower dimensional space with PCA:

1. Let $x = [x_1, x_2, ...x_n]$ be a data vector with $x \in R$.
2. Select a basis, with the set of basis vectors being $u = [u_1, u_2, ...u_n]$. An orthonormal basis has the usual properties $u_i \cdot u_i = 1$, and $u_i \cdot u_j = 0$ for $i \neq j$.
3. Select a center. $\bar{x}$ defines offset of the space.
4. The best coordinates in lower dimensional space are defined by dot-products as

$$(z_1, z_2, ....z_k), \quad z_i = (x - \bar{x}) \cdot u_i. \tag{1}$$

5. The requirement is: find a direction of $z_i$ that maximizes the variance and minimize the mean square error (mse).

PCA transforms the data to a new coordinate system such that the direction with the greatest variance lies on the first coordinate called the first principal component (factor), the second greatest variance on the second coordinate, and so on. This situation is shown in Figure1(a) and Figure1(b).

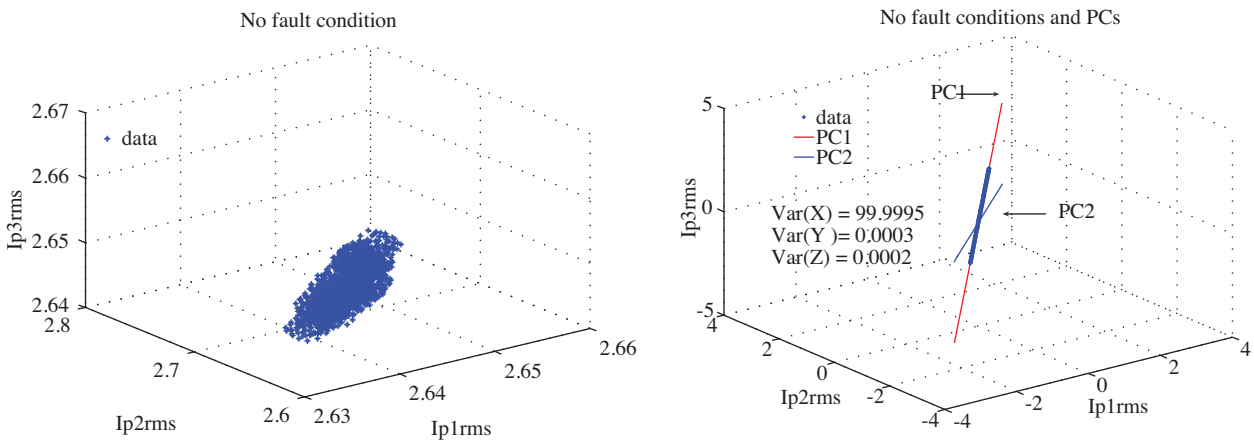


**Figure 1.** (a) A collection of unconverted, trivariant data. (b) The principal axes after data rotating the coordinate frame in order to maximize the variance of projections.

In Figure1(a), the left side shows an example of unconverted no-fault data points. Figure1(b) shows the data's principal axes after reduction to such a domain that has maximum variance; PC1 and PC2 label the principal components. Ip1rms, Ip2rms and Ip3rms are the true rms values of the line currents during no fault condition in Figure 1(a). In Figure 1(b), data is the points that are converted to PCs.

**B)** The basic PCA algorithm used in this paper is defined in the following steps

1. Read the data matrix of $Y$ by $m \times n$ $(20 \times 3)$. The sampling frequency is chosen as 1000 Hz. and it yields to 20 samples in per data window. Three phase line currents are stored as a $20 \times 3$ matrix.

2. Re-centering procedure is performed by subtracting the mean value from each row of $Y$ by computing

$$Y_c = Y - \bar{Y}. \tag{2}$$

3. The covariance matrix is computed by the equation

$$\sum = \frac{1}{m}\sum_{i=1}^{m}(Y_c - \bar{Y})(Y_c - \bar{Y})^T \tag{3}$$

4. Then eigenvalues and eigenvectors of $\sum$are calculated.

5. Select the $k^{th}$ eigenvectors with maximal eigenvalues (principal components). Note that covariance matrix can be really big; therefore finding eigenvectors may require much computer time. To overcome this problem, singular value decomposition (SVD) is used to calculate the $k^{th}$ eigenvectors. Section 2.1 gives a brief description of SVD calculation.

## 2.1. SVD calculation

The general SVD form is defined as

$$Y = WSV^T \tag{4}$$

Here, $Y$ is the data matrix, one row per data point. As stated above, $Y$ contains acquired 3 phase current samples. $W$ is an $m \times m$ weight matrix of eigenvectors of $YY^T$ – coordinate of $x^i$ in eigenspace. $S$ is a singular value, diagonal matrix (in our setting, each entry is an eigenvalue $\lambda_i$), i.e, $n$ diagonal elements contains of square root of the eigenvalues of $Y^TY$ or $YY^T$, all other elements are zero. $V^T$ is a singular vector matrix (in our setting, each row is and eigenvector $v_j$), i.e., rows of $V$ contains the coefficients of the principal components.

The product $WS$ contains scores of the principal components that amounts to the contribution of each observation to the principal components. The relation between SVD and eigenvalues is achieved through the relations

$$\begin{aligned} YY^T &= (WSV^T)(WSV^T)^T = WSV^TVSU^T = US^2U^T \\ Y^TY &= (WSV^T)^T(WSV^T) = VSW^TWSV = VS^2V^T \end{aligned} \tag{5}$$

Matrices $W$ and $V$ are orthogonal so $W^T = W^{-1}$. This means that $W$ and $V$ can be calculated as the eigenvectors.

## 2.2. Error vector calculation

The first stage is data manipulation. The data $Y$ is constructed in a dynamic way under normal working conditions from the samples of the system inputs as

$$Y = \left[y_{k-l+1}^T, y_{k-l+2}^T, \ldots, y_k^T\right]^T, \tag{6}$$

where $l$ denotes system order and $y$ contains each phase current samples of length $k$. Since different variables in engineering systems usually use different units, the columns of $Y$ usually need to be scaled; so they have zero mean and unity variance.

In the second stage, off-line stage, the covariance matrix is calculated by using auto scaled matrix as

$$Cov = \frac{Y^T Y}{n-1}, \tag{7}$$

where $Y$ shows auto scaled data matrix. Offline PCA training covers extensive laboratory experiments on specially designed IM. Offline experiments include healthy working conditions, stator winding faults, rotor bar failures, and bearing faults. The calculated rms values of each line currents are recorded for PCA offline training.

To calculate principal components (PCs), the eigenvectors and eigenvalues of the covariance matrix have been computed and arranged in order of decreasing eigenvalues. The eigenvectors of the auto scaled covariance matrix are called PCs and they are used for residual generation purposes.

In the last stage, on-line residual generation stage, each new observation vector (acquired phase currents in per data frame) is auto scaled using the means and variances obtained in the off-line stage and projected on to the principal component subspace. Then a residual vector at discrete time $k$ is calculated, using a few principal components (PCs) as

$$e_k = \|Y_m - \wedge Y\|^2 = \left\|(I - W_1 W_1^T) Y_m\right\|^2. \tag{8}$$

Here, $\|\|^2$ denotes the norm of a vector, which calculates the square value of the largest column sum of $e_k$.

In a different way, the residual vector $e$at discrete time$k$ is calculated by using a few PCs related to the error matrix $W_2$ as

$$e_k = \left\|W_2 W_2^T Y_m\right\|^2 \tag{9}$$

where $Y_m$ shows measurement vector and $\hat{Y}$ is called the prediction of the measurement vector and indices $\boldsymbol{k}$ refers to phases A, B, and C (or phases 1, 2, and 3). Selecting procedure of PCs is simple. PCs, which have variance 80% of the total variance, can be selected. A threshold value of 80% variance is enough to reconstruct the original data with an acceptable error.

After calculating the residual vectors, a fault isolation technique is applied. Threshold based fault isolation techniques may not work well due to power system dynamics. So, classification techniques, or reasoning based fault isolation methods should be used. If the proposed overall protection system is trained against the power system disturbances, the protection algorithm will remain stable in case of any disturbance. In this study, no power system disturbance is assumed.

The error vector $e_k$ is applied to the ANN network as an input. The ANN network produces decisions as no fault, stator winding fault, bearing fault, and broken rotor bar fault. Section 3 gives a brief background for ANN structures.

## 3. ANN structure for fault identification and classification

ANN is used for fault identification and classification. A feed forward back propagation neural network is a multilayer network which consists of an input layer, a hidden layer and an output layer. A three-stage network was formed, comprising a feed-forward for input pattern training, back propagation for computing calculated error, and weight adjustment based on the error calculation. Activations flow from the input layer through the hidden layer, then to the output layer. A back propagation network typically starts out with a random set of weights. In feed-forward stage, the input neuron receives the input signal and fires it to every hidden neuron.

Upon receiving the signal from the input neuron, the hidden neuron computes the activation and the result fires to the output layer.

At the output layer, the output neuron computes the activation to obtain the net output. In the second stage, the back propagation of error stage computes the error by comparing the net output with the desired or target value. From the error, the error gradient at the hidden and the output neurons are calculated and new weights are determined. The back propagation network updates its weights incrementally until it produces more accurate predictions, upon which the network stabilizes. This is carried out in the last stage of the network, the weight-update stage.

The proposed network structure is as follows.

*i) Training Set*

The input/output set is the data obtained from the experiment stage and pre-processes. This stage has numerous set of data obtained from the real world. Approximately 60 different laboratory tests are performed in laboratory environment. Forty (40) of them are used for training procedure for PCA and ANN and the rest is used for testing procedures. The calculated error vectors by using equation (9) and associated outputs are used for training procedure. The outputs have binary decisions such as 1/0. Table 1 shows the outputs and decisions produced in ANN.

**Table 1.** Network outputs for various fault conditions. (a) Shows the network outputs for the "no fault" condition. (b) Shows network outputs for the "stator winding fault" condition. And (c) shows network outputs for multiple fault conditions.

| | Outputs | Decisions |
|---|---|---|
| No fault | 1 | True |
| Stator windings fault | 0 | False |
| Bearing fault | 0 | False |
| Rotor bar fault | 0 | False |

(a)

| | Outputs | Decisions |
|---|---|---|
| No fault | 0 | False |
| Stator windings fault | 1 | True |
| Bearing fault | 0 | False |
| Rotor bar fault | 0 | False |

(b)

| | Outputs | Decisions |
|---|---|---|
| No fault | 0 | False |
| Stator windings fault | 1 | True |
| Bearing fault | 1 | True |
| Rotor bar fault | 0 | False |

(c)

ii) *Test Set*

The Test Set is a collection of input and output values that are used to assess or test the network performance. Usually, the training set is a randomly selected subset of the testing set. The testing set is the complete set of data and obtained from real time working conditions.

iii) *Learning Rate*

Learning rate is a guideline, a scalar parameter, to determine the analogous changes that occur in the weights of each circle as the network undergoes training.

iv) *Momentum Factor*

The momentum factor is added to enhance the speed of network training. By adding the momentum factor, the weight changes according to the direction of the current gradient descent.

## 4. Number of input neuron and hidden neuron

The number of input neuron and hidden neuron is a critical factor for a good training. As there is no specific method on how to determine the number of input neuron and hidden neurons in a network training, trial and error is used as guidelines in determining the number of hidden neuron in this work.

The basic architecture of the fault identification unit with 3 inputs and 4 outputs is shown in Figure 2.

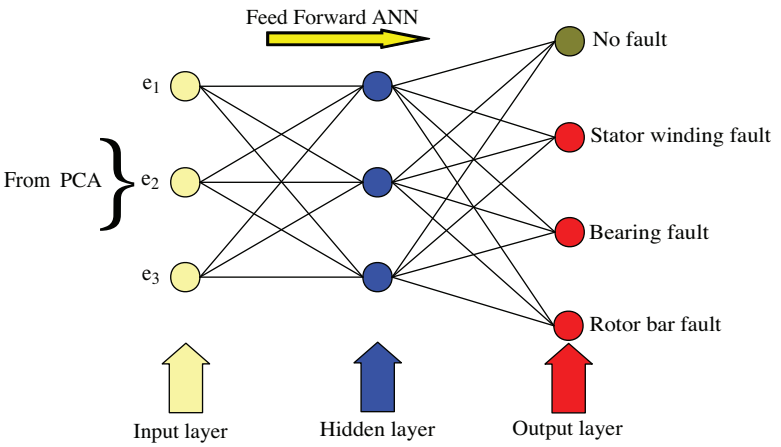


**Figure 2.** Basic ANN architecture for fault detection, incorporating 3 inputs and reporting with four outputs.

As illustrated in Figure 2, the suggested ANN network has one input layer with 3 neurons (i.e. fed by dynamical PCA algorithm), a hidden layer with 3 neurons and an output layer with 4 neurons. The input and hidden layer have tangent sigmoid activations. The nodes in adjacent layers are fully connected.

Figure 3 shows the flowchart of the proposed fault detection and identification technique. The input vectors are defined as in equation (12).

The overall ANN calculation used in this paper is defined as

$$Y_i = [e_1 \ e_2 e_3]_{20\times 3}\,. \tag{10}$$

The input vector $Y_i$ is a $20\times 3$ matrix and is output of the PCA algorithm. The hidden neuron is defined as

$$\begin{aligned} Z_{inj} &= v_{oj} + \sum X_i v_{ij} \\ Z_j &= f(Z_{inj}), \end{aligned} \tag{11}$$

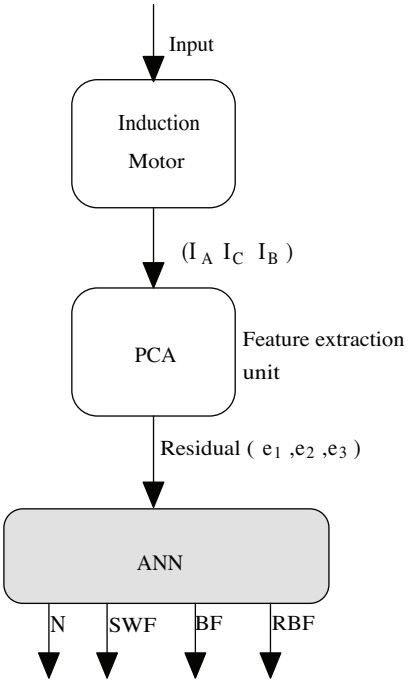


**Figure 3.** A complete fault identification and detection flowchart for motor protection. At the output of the ANN, N denotes normal operation, SWF denotes stator winding fault, BF denotes bearing fault, and RBF denotes rotor bar fault.

where $Z_j$ is the output of the hidden unit and input of the output unit and $i, j = 3$. $v_{oj}$ is the threshold weights of back propagation.

The output neuron is defined as

$$\begin{aligned} Out_{inj} &= w_{oj} + \sum Z_i w_{ij} \\ Out_j &= f(Out_{inj}). \end{aligned} \tag{12}$$

The network error at the $t^{th}$ iteration is defined as

$$\begin{aligned} \delta_k &= (t_k - y_k) f'(Y_{inj}) \\ \Delta w_{jk}(t) &= \lambda \delta_k Z_j + \alpha \Delta w_{jk}(t-1) \\ \Delta w_{0k}(t) &= \lambda \delta_k + \alpha \Delta w_{0k}(t-1). \end{aligned} \tag{13}$$

Here, $t_k$ is the expected output, $Out_k$ is the output, $f'(Out_{inj})$ is the derivation of the output through activation function, and $\Delta w_{0k}$ is the total error at time instant $k$.

The activation is computed on the hidden neuron based on the output error as

$$\begin{aligned} \delta_{inj} &= \sum_{k=1}^{m} \delta_k w_{jk} \\ \delta_j &= \delta_{inj} f'(Z_{inj}) \\ \Delta v_{ij}(t) &= \lambda \delta_k X_i + \alpha \Delta v_{ij}(t-1) \\ \Delta v_{0j}(t) &= \lambda \delta_j + \alpha \Delta v_{0j}(t-1). \end{aligned} \tag{14}$$

In equation (14), $\Delta v_{0j}$ is the back-propagation variation of the threshold weights, $\delta_j$ is the back-propagation error at the $j^{th}$ layer and $t^{th}$ iteration.

The weights are updated using the relations

$$\begin{aligned} w_{jk}(new) &= w_{jk}(old) + \Delta w_{jk} \\ v_{ij}(new) &= v_{ij}(old) + \Delta v_{ij}. \end{aligned} \tag{15}$$

In the above equations, $\alpha$ is momentum and $\lambda$ is the learning coefficient. This procedure, comprising equations (10)–(15), is repeated until the desired rms error is reached. Table 2 shows the initial values of the ANN. (*The number of hidden neurons can be controlled by the produced software in C++ environment. The number of 3 is found suitable for real time experiments with an acceptable error. The higher number of hidden neurons for instance 6, the lower overall error is calculated.)

**Table 2.** Initial ANN values.

| | |
|---|---|
| Input neurons | 3 |
| Hidden neurons* | 3 |
| Output neurons | 4 |
| Learning rate ($\lambda$) | 0.001 |
| Momentum ($\alpha$) | 0.9 |
| Max. Epochs | 500 |

# 5. Real time studies

A custom-built, three-phase induction motor (1 kVA, 380 V, 2.8 A, 4 poles) has been used for laboratory experiments to test the suggested fault protection algorithm. Different internal faults within the motor (i.e. insulation faults) are formed in the laboratory. Stator line currents are acquired with a sampling frequency of 1000 Hz, which corresponds to 20 samples per cycle. A sampling frequency of 1 kHz is found suitable to implement the whole algorithm. True rms values of the line currents are calculated in each window interval and they are applied as inputs of the PCA algorithm to get the features from the three-phase currents. The outputs of the PCA are the feature vectors representing normal working condition, abnormalities in the stator windings, rotor bar failures, and bearing faults. The simulation time is set to 2 sec for all real time experiments.

The following figures show the result of real time experiments.

## 5.1. No fault condition

A number of experiments with different load conditions are performed in this section. The calculated rms values from instantaneous line currents are used as offline training procedure for PCA algorithm. Then the residuals (error vector) calculated by equation (9) are the inputs of the ANN for training procedure. In case of no fault condition, the magnitude of the error vector is very low (assumed zero) as seen in Figure 4.

In Figure 4, the first row represents line currents of the motor and second row represents the calculated error vectors during no fault condition. The algorithm interprets the magnitudes of the error vectors as zero during no fault condition since the magnitudes have a value of between $10^{-3}$–$10^{-4}$ approximately. Then these error vectors $(e_A, e_B, e_C)$ are used as input functions of ANN. The output of ANN will produce "*no fault*" with these inputs.

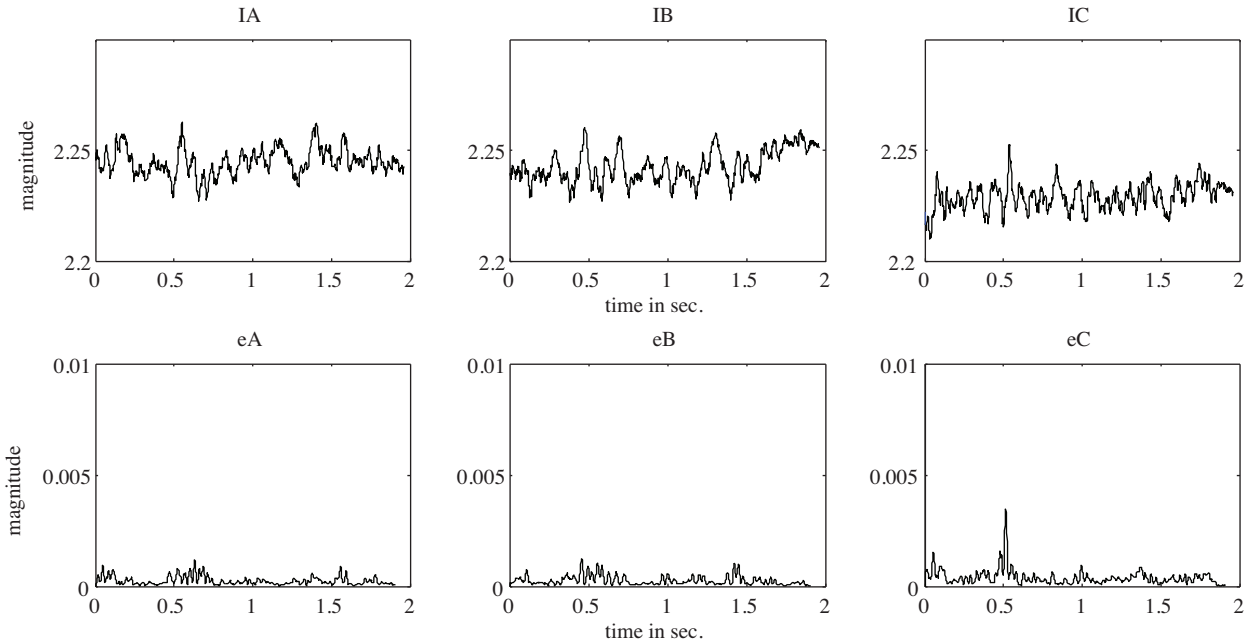


**Figure 4.** Stator line currents and calculated error vectors (output of PCA) during no fault condition.

## 5.2. Stator winding faults

All stator winding faults are implemented by using a fault resistance $F_R$ to limit the short circuit current and to simulate the high impedance faults. Turn-to-turn or turn-to-earth fault is instantaneously formed by an electro-mechanical relay and a fault switch, $SW$. Figure 5 shows the fault inception scheme and 4-pole winding layout.

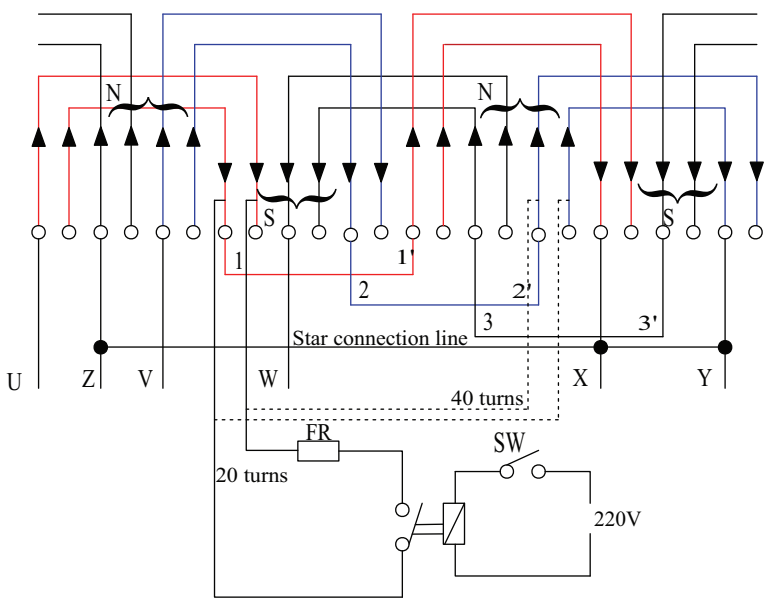


**Figure 5.** Winding layout of the custom built motor and fault inception scheme. Red lines denote faulty phase information. The blue lines denote phase C information, and is used in testing the algorithms.

A number of turn-to-turn or turn-to-earth faults are done in stator windings. In this work, the faulty phase information (A Phase, denoted by red lines) is used for training the PCA and ANN. Another, C phase information (denoted by blue lines) is used for testing for these algorithms. Fault resistance, $FR$, is chosen as 0.5 Ω, 1 Ω, 2 Ω and 2.5 Ω to simulate possible insulation faults in phase windings.

Figure 6 shows the PCA outputs (ANN inputs) for 20 turns short-circuited in phase A. As seen in Figure 6, the magnitudes of error vectors are much higher than the magnitudes of error vectors during normal operating condition. Since the overall experimental set up is a three phase system, two phase currents are affected during the internal fault in only one phase.

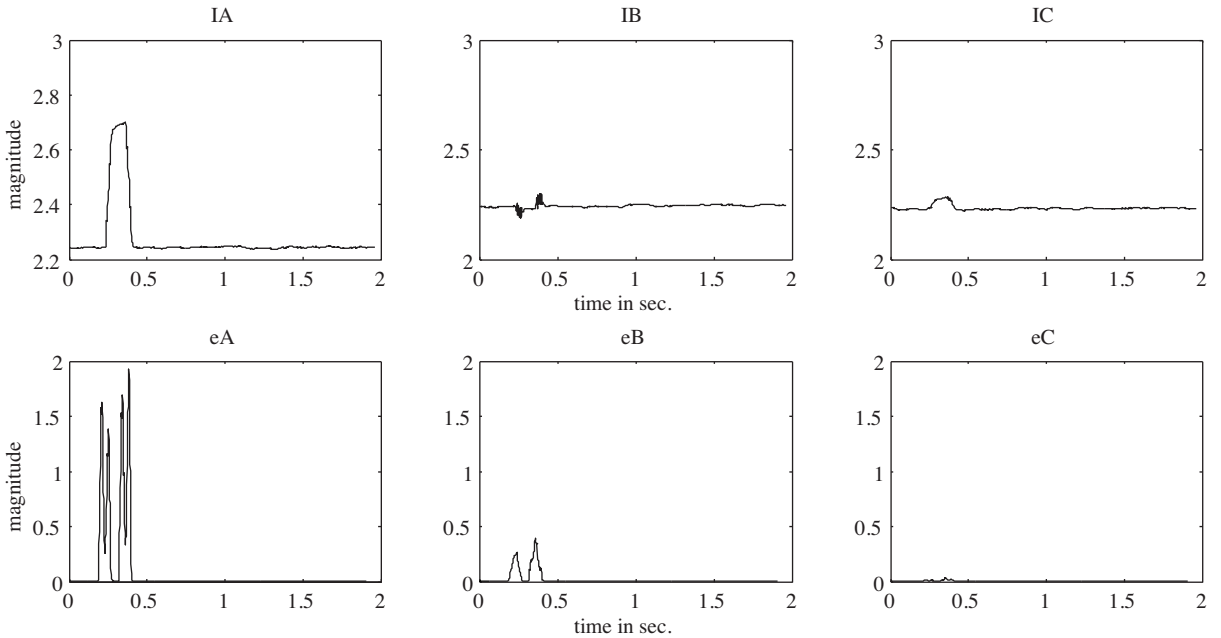


**Figure 6.** Stator line currents and calculated error vectors (output of PCA) during internal fault in A Phase.

## 5.3. Start-up condition

Since the start-up condition is not a fault, the proposed protection algorithm should not report a fault during the start-up process. Towards this need, PCA algorithm is trained for start-up condition and the related output of ANN interprets this situation as normal operating condition. Unlike the error vectors during internal faults, all error vectors have a spikes and higher magnitudes as seen in Figure7. During the start-up process, the first ANN output of "no fault" is activated.

## 5.4. Bearing fault condition

This condition is tested by using an intentionally damaged bearing, pictured in Figure 8. With this bearing the phase currents (rms values) did not change significantly but the output of the PCA exhibited distinctive features. As such, the ANN algorithm interpreted this situation as a bearing fault.

Figure 9 shows the stator line currents and calculated error vectors during the bearing fault condition.

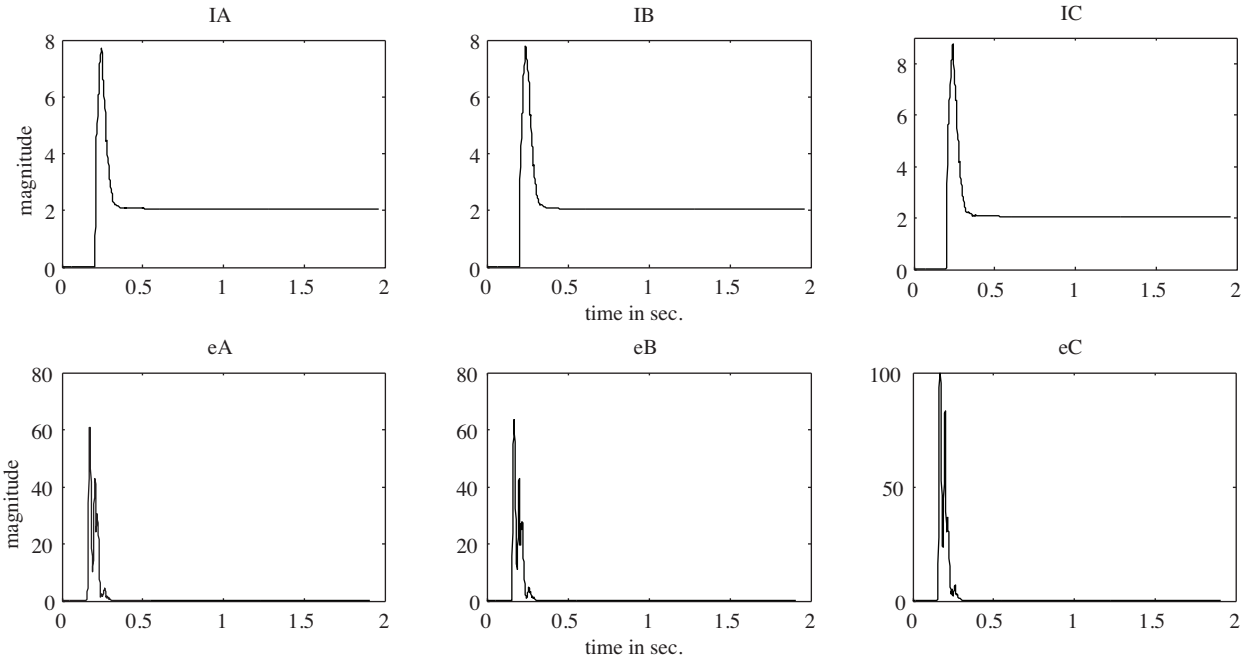


**Figure 7.** Stator line currents and calculated error vectors (output of PCA) during start-up process.

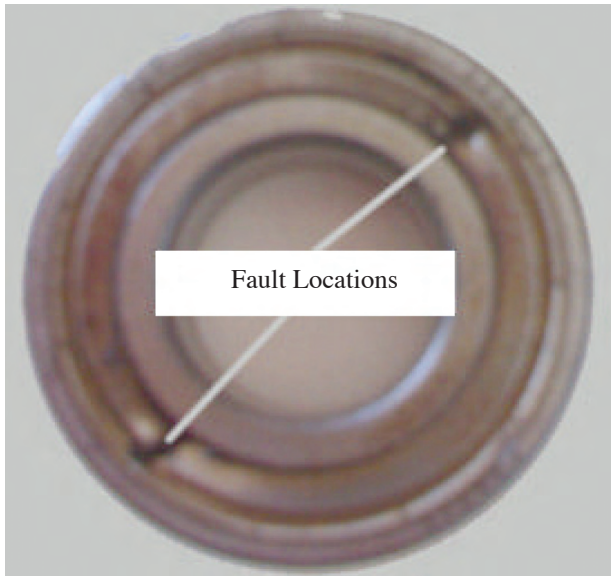


**Figure 8.** Artificially created bearing fault.

## 5.5. Broken rotor bar fault

Two identical rotors are used for real time experiments, one for healthy conditions, the other (having a broken bar) used for testing rotor bar faults. Figure 10 shows the rotor with a broken bar.

Figure 11 shows the stator line currents and calculated error vectors during rotor bar fault condition. Unlike the bearing fault condition, magnitudes of the error vectors are higher than the bearing rotor fault condition. Therefore the ANN algorithm interprets this situation as rotor bar fault condition.

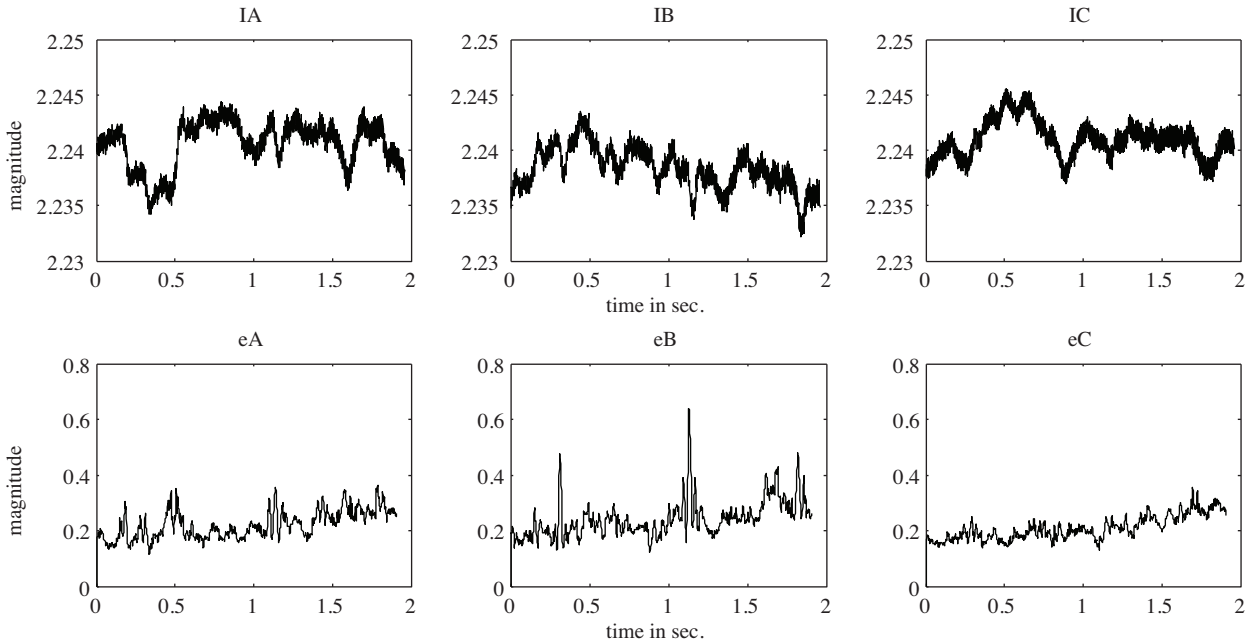


**Figure 9.** Stator line currents and calculated error vectors during bearing fault condition.

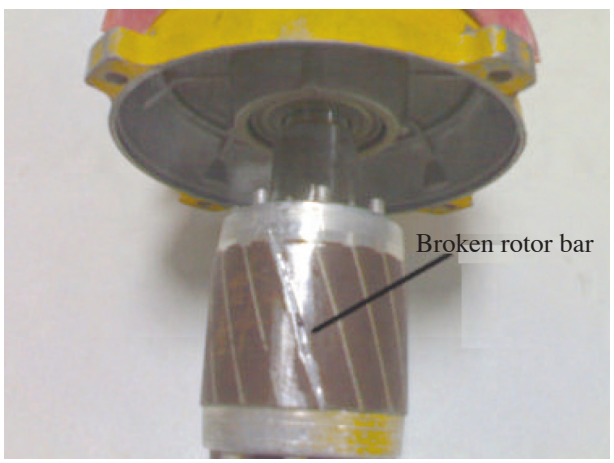


**Figure 10.** Photo graph of a broken rotor.

**Table 3.** The magnitudes of error vectors during possible working conditions.

| Working Conditions | eA | eB | eC |
|---|---|---|---|
| No fault | $\approx 0.001$ | $\approx 0.001$ | $\approx 0.001$ |
| Stator winding fault | 1.8 | 0.5 | $\approx 0.1$ |
| Bearing fault | 0.4 | 0.6 | 0.4 |
| Rotor bar fault | 0.5 | 1.2 | 0.9 |

During the no fault (healthy) condition, magnitudes of eA, eB and eC were approximately less than or equal to 0.001. If any of the magnitude exceeds these values, the ANN unit decides it as "faulty condition" then classifies the fault. During stator winding fault condition, the related magnitudes are higher than the no fault condition, especially in faulty phase A. For bearing fault condition, the related magnitudes were nearly

the same or higher than the "no-fault" conditions. Without real-time experiments, these values were expected to be the same; present experiments show there are slight changes in magnitudes.

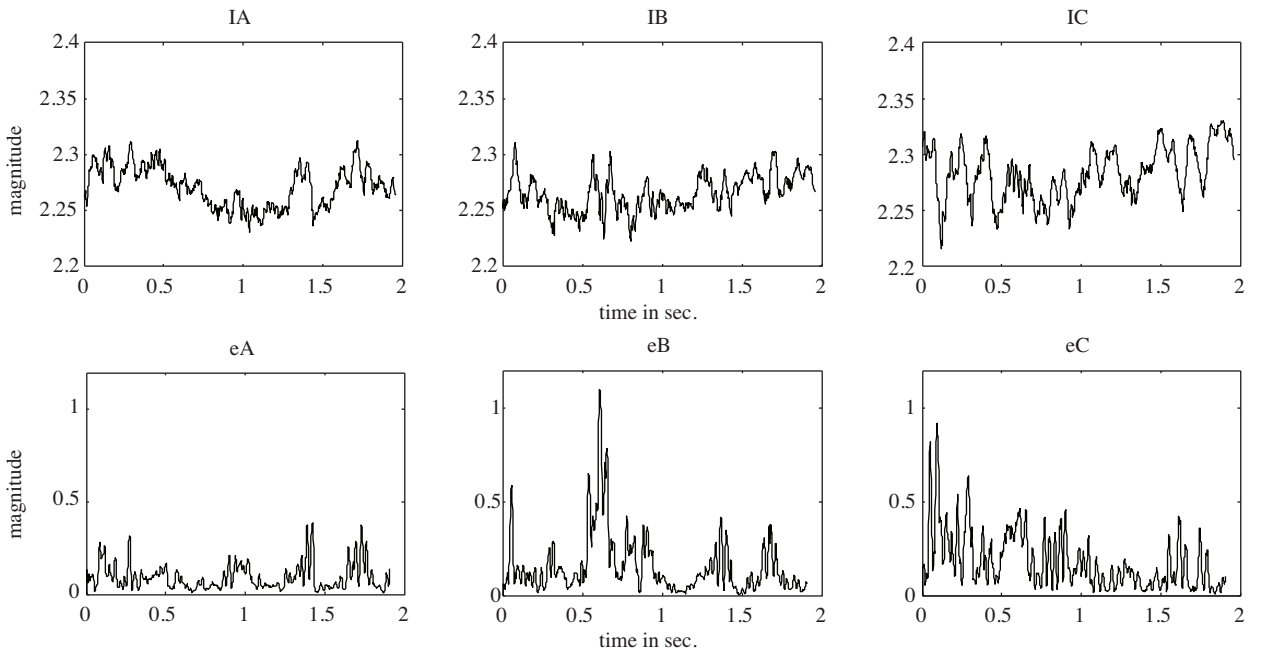


**Figure 11.** Stator line currents and calculated error vectors during rotor bar fault condition.

Finally, during the rotor bar fault condition, magnitudes of the two error vectors are near and the third one is about half of them. In case of two bars broken rotor test, the magnitudes of the two are still near and higher than the third one. Then the ANN unit successfully identifies these working conditions.

Broken rotor bar fault condition is tested while induction motor is unloaded. As stated in the Introduction, if the machine is unloaded, classical frequency based approaches fail to identify the fault due to the frequencies associated with the broken rotor bars will overlap the supply frequency. As seen in Figure 11, even the machine is unloaded; the proposed protection algorithm is successfully able to identify the broken rotor bar fault.

Figures 12 and 13 show the fundamental and subharmonic frequencies during no-load condition, respectively without rotor bar fault and with rotor bar fault.

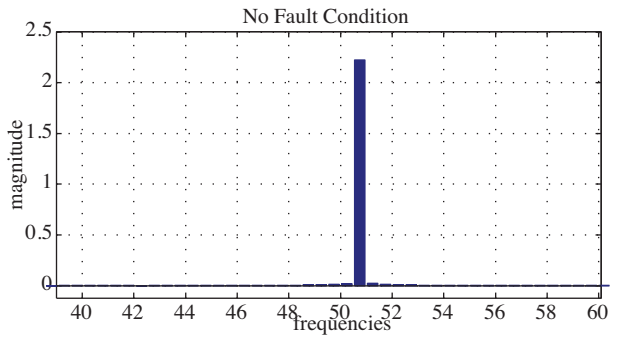


**Figure 12.** Fundamental and sub harmonics during no-load and healthy condition.

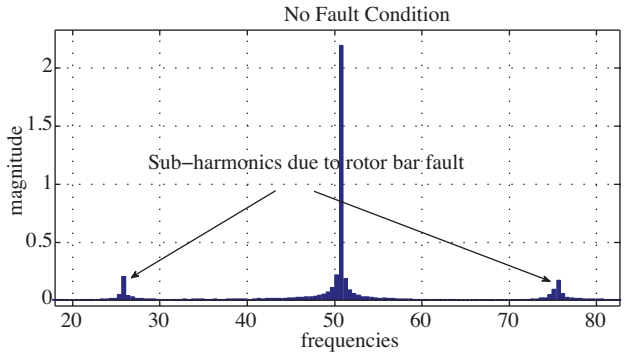


**Figure 13.** Fundamental and sub harmonics during no-load and rotor bar fault condition.

As seen in Figure 13, frequency based techniques like FFT can detect the subharmonics caused by rotor bar fault; but since they have low magnitudes and can also be produced by oscillating load torques, they can not be used as distinctive features for future analysis. Similar results are obtained in case of broken two rotor bars. The ANN unit successfully identifies the phenomena as rotor bar fault.

To discriminate normal operation and faulty conditions, data acquisition and controller circuit are used. The controller circuit produces digitally 1/0 (0–5 V) for SSRs to disconnect the motor from supply. Schematic representation of the tripping circuit is given in Figure 14.

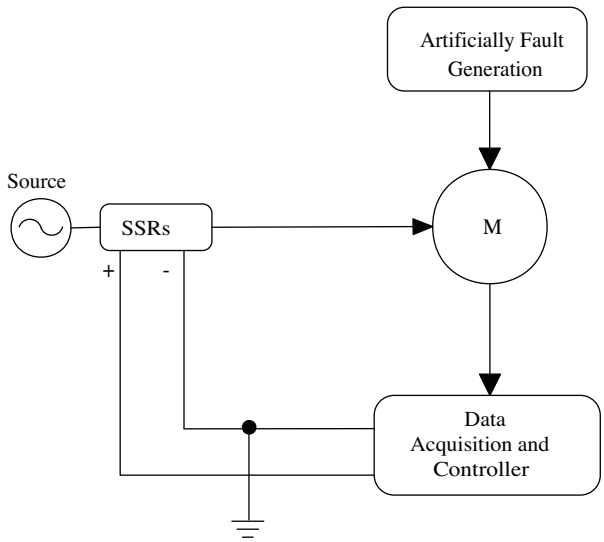


**Figure 14.** Schematic representation of the tripping circuit.

# 6. Conclusion

This paper presents a novel application of PCA and neural network for a complete three phase induction motor protection scheme. The protection algorithm covers stator winding faults, bearing faults, and broken rotor bar faults. These faults are tested on a specially designed induction motor in laboratory environment. If any of these faults is occurred, the controller unit sends a trip signal to SSRs and motor is then stopped.

The suggested protection algorithm is based on true rms values of three phase stator currents. These currents are first preprocessed by PCA to distract distinctive features and then supplied as input variables to

ANN for classifying the faults. The method is tested in different faulty and operating conditions, and its results are compared with those obtained from the classical Fourier analysis of the stator current in steady state.

The suggested protection algorithm doesn't require any additional hardware sensors to be installed in the machine, knowledge of machine design details or special wiring constrains. In other words, a resident expert is not required. The proposed technique has been verified using real time experimental test results.

The authors believe that this technique presents a powerful tool which can be utilized in a future research to predict a faulty motor remaining life and provide fault mitigation strategy for this type of faults.

# References

[1] Venkataraman, B.; Godsey, B.; Premerlani, W.; Shulman, E.; Thaku M; Midence, R., "Fundamentals of a Motor Thermal Model of Its Applications in Motor Protection", 2005 58th Annual Conference for Protective Relay Engineers, 2005, pp. 127–144.

[2] J. F. Martins, V. Fernão Pires, and A. J. Pires, "Unsupervised Neural-Network-Based Algorithm for an On-Line Diagnosis of Three-Phase Induction Motor Stator Fault", IEEE Trans. On Industrial Electronics, Vol. 54, No. 1, February 2007.

[3] Farag, S.F.; Bartheld, R.G.; Habetler, T.G., "An Integrated, On-line, Motor Protection System, Industry Applications Society Annual Meeting, 1994, pp. 117–122.

[4] Bayindir, R.; Sefa, I.; Colak, I.; Bektas, A., "Fault Detection and Protection of Induction Motors Using Sensors", IEEE Transactions on Energy Conversion, Vol. 23, Issue 3, 2008, pp. 734–741.

[5] A. Stavrou, H. G. Sedding, and J. Penman "Current Monitoring for Detecting Inter-Turn Short Circuits in Induction Motors," IEEE Trans. On Energy Conversion, vol. 16, March 2001.

[6] J. Penman, H. G. Sedding B. A. Lloyd, and W. T. Fink "Detection and location of interturn short circuits in the stator winding of operating motors," IEEE Trans. On Energy Conversion, vol. 9, pp. 652–658, Dec. 1994.

[7] G. M. Joksimovic and J. Penman "The Detection of Interturn Short Circuits in the Stator Windings of Operating Motors," IEEE Trans. On Industrial Electronics, vol. 47, Oct. 2000.

[8] S. Nandi and H. A. Toliyat "Novel Frequency –Domain-Based Technique to Detect Stator interturn Faults in Induction Machines Using stator–Induced Voltages After Switch Off," IEEE Trans. Industrial Applications, vol. 38, Jan/Feb. 2002.

[9] S. Nandi, H. A. Toliyat, and X. Li "Condition Monitoring and Fault Diagnosis of Electrical Motors-A Review," IEEE Trans. On Energy Conversion, vol. 20, pp.719–729, Dec. 2005.

[10] Ahmet Sayed, Chia-Chou Yeh, Nabeel A. O. Demerdash, Behrooz Mirafzal, "Analysis of Stator Winding Inter-Turn Short-Circuit Faults in Induction Machines for Identification of the Faulty Phase", IEEE 41st IAS Annual Meeting Conference, Volume 3, 8–12 Oct. 2006, pp. 1579–1524

[11] Rajesh Patel, S P Gupta, and Vinod Kumar, "Real-Time Identification of Distributed Bearing Faults in Induction Motor", PEDES '06. International Conference on Power Electronics, Drives and Energy Systems, 12-15 Dec. 2006, pp. 1–5.

[12] M. F. Cabanas, M. G. Melero, and G. A. Capolino, "A new methodology for applying the FFT to induction machine on-line diagnosis," in *Proc.Int. SDEMPED*, Gijon, Spain, Sep. 1999, pp. 537–543.

[13] A. Bellini, F. Filippetti, G. Franceschini, C. Tassoni, and G. B. Kliman, "Quantitative evaluation of induction motor broken bars by means of electrical signature analysis," *IEEE Trans. Ind. Appl.*, vol. 37, no. 5, pp. 1248–1255, Sep./Oct. 2001.

[14] F. Filippetti, G. Franceschini, C. Tassoni, and P. Vas, "AI techniques in induction machines diagnosis including the speed ripple effect," *IEEE Trans. Ind. Appl.*, vol. 34, no. 1, pp. 98–108, Jan./Feb. 1998.

[15] R. R. Schoen and T. G. Habetler, "Evaluation and implementation of a system to eliminate arbitrary load effects in current-based monitoring of induction machines," *IEEE Trans. Ind. Appl.*, vol. 33, no. 6, pp. 1571–1577, Nov./Dec. 1997.

[16] J. F. Watson, K. S. Gow, and W. T. Thomson, "Non-invasive instrumentation for on-line management and monitoring of electrical plant," in *Proc. Inst. Elect. Life Manage. Power Plants*, 1994, pp. 48–56.

[17] M. Negrea, P. Jover, and A. Arkkio, "A comparative investigation on the reliability and accuracy of different diagnostic media when attempting to identify specific faults in an induction motor," in *Proc. SPEEDAM*, Capri, Italy, May 16–18, 2004, pp. 809–814.

[18] Jose A. Antonino-Daviu, Martin Riera-Guasp, José Roger Folch, and M. Pilar Molina Palomares, "Validation of a New Method for the Diagnosis of Rotor Bar Failures via Wavelet Transform in Industrial Induction Machines", IEEE Trans. On Industry Applications, Vol. 42, No. 4, July/August 2006, pp. 990–996.

[19] A. J. M. Cardoso, S. M. A. Cruz, J. F. S. Carvalho, and E. S. Saraiva, "Rotor cage fault diagnosis in three-phase induction motors by Park's vector approach," in Proc. IEEE Ind. Appl. Conf., 1995, vol. 1, pp. 642–646.

[20] A. J. M. Cardoso, S. M. A. Cruz, and D. S. B. Fonseca, "Inter-turn stator winding fault diagnosis in three-phase induction motors, by Park's vector approach," IEEE Trans. Energy Conv., vol. 14, pp. 595–598, Sep. 1999.

[21] R. Burnett, J. F. Watson, and S. Elder, "The application of modern signal processing techniques to rotor fault detection and location within three phase induction motors," Eur. Signal Process. J., vol. 49, no. 1, pp. 57–70, Feb. 1996.

[22] J. F. Watson and N. C. Paterson, "Improved techniques for rotor fault detection in three-phase induction motors," in Conf. Rec. IEEE-IAS Annu. Meeting, Oct. 12–15, 1998, vol. 1, pp. 271–277.

[23] E. Kilic, O. Ozgonenel, A.E. Ozdemir, "Fault Identification in Induction Motors with RBF Neural Network Based on Dynamical PCA", The IEEE International Electric Machines and Drives Conference (IEMDC 2007), 3–5 May, 2007, Antalya.

[24] Haiging W., S. Zhihuan and L. Ping, "Improved PCA with optimized sensor locations for process monitoring and fault diagnosis", Proceeding of the $39^{th}$ IEEE Conference on Decision and Control, pp 4353–4358, Sydney, Australia, December, 2000.